Conducting polymers under pressure: synchrotron x-ray determined structure and structure related properties of two forms of poly(octyl-thiophene)

J Mårdalen†, E J Samuelsen‡, O R Konestabo‡, M Hanfland§ and
M Lorenzen§

† SINTEF Applied Physics, N-7034 Trondheim, Norway
‡ Department of Physics, NTNU, N-7034 Trondheim, Norway
§ ESRF, F-38043 Grenoble Cédex, France

Abstract. Synchrotron x-ray diffraction from poly(3-octylthiophene) and poly(3,3′-dioctyl-2,2′-bithiophene) revealed that the structures of these two polymers remain different under hydrostatic pressure despite their similar chain configuration. The a-axis of poly(octyl-thiophene) is considerably more compressible than its b-axis, and poly(octyl-thiophene) is more compressible along both these directions than poly(dioctyl-bithiophene). The differences in compressibility corroborate with the planar chain model of poly(octyl-thiophene) and the chain twist model of poly(dioctyl-bithiophene), but with a reduction in the chain twist angle under pressure for the latter. The spectral shift caused by variation of temperature (thermochromism) is compared with the spectral shift caused by pressure. From the shifts of the *band edge* and the behaviour of the overall peak shape it is argued that these two effects are associated with different structural aspects: whereas thermochromism is related to a two phase situation, the shift caused by pressure is related to an increased interchain wave function overlap.

1. Introduction

Conjugated polymers remain a challenging field of basic materials studies, because the materials combine several properties that are still only partly understood. In their undoped state the materials are organic semiconductors, whose energy gap (E_g) is determined by the presence of orbital conjugation (and thus of atomic orbital overlap) along the polymer main chains. For normal alkyl-substituted poly(thiophene)s (PATs) the gap amounts to about two eV at ambient temperatures, giving rise to the characteristic red colour of PATs. The gap is, however, found to be temperature dependent for normal PATs [1, 2], so that PATs change their colour to yellow at elevated temperatures ('thermochromism'). For poly(octyl-thiophene) (POT) the transition temperature is about 150 °C. On the other hand in a polymorphic form of POT called PDOT₂, characterized by a regular *head-to-head/tail-to-tail* sequence (see later) along the chain, thermochromism is absent [3].

Hydrostatic pressure is known to modify considerably several properties of conjugated polymers. For poly(acetylene) (PA) [4], poly(paraphenylene) (PPP) [5] and PATs [6, 7] application of pressure gives rise to a gap lowering (redshift). Also photoluminescence and photoabsorption are influenced by pressure [6, 8]. Similarly, conductivity increases in both undoped and doped materials have been observed under moderate pressure [7, 9], and shift and broadening of Raman lines and also appearance of new lines indicate that certain

configurational changes may take place due to the pressure [6, 7]. Of particular interest is that at pressure above 1.4 GPa the imposed redshift of PATs is sufficient to completely suppress the thermochromism.

Based on these facts we found it very desirable to perform structural studies of POT and PDOT$_2$ under pressure. A previous preliminary study using a white x-ray synchrotron beam [10] is at some variance with the results from the present study. The discrepancies are believed to be due to inaccuracies in the experimental setup and some sample deterioration associated with excess heat load in the previous study.

2. The structure of poly(octyl-thiophene)s

Poly(3-alkyl-thiophene)s (PATs) are partially crystalline/partially amorphous materials. Their molecular and crystalline structure at ambient pressure have been well established during recent years with a reasonable degree of consensus [11]. Figure 1 shows the orthorhombic unit cell employed, for the case of A being octyl (POT).
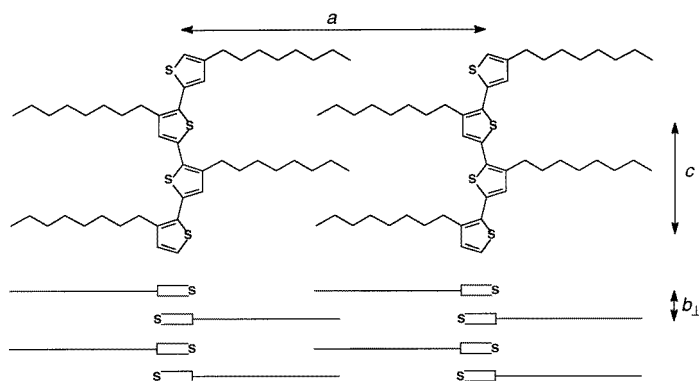

Figure 1. Simplified pseudo-orthorhombic view of the POT crystalline structure projected along the $b_\perp$ (upper) and c (lower) directions. For simplicity $b_\perp$ will be used as a (pseudo-) unit cell parameter denoting the distance between neighbouring poly(thiophene) chains stacked on top of each other. It should however, be kept in mind that a parallel chain displacement along the c direction, implying a monoclinic unit cell with $b = b_\perp / \sin \alpha$, has been reported [12]. $a = 20.3 \pm 0.1$ Å, $b = 4.80 \pm 0.06$ Å, $c = 7.85 \pm 0.04$ Å, $\alpha = 52 \pm 1°$ and $b_\perp = 3.76 \pm 0.03$ Å for POT at ambient pressure.

The POT used in the present study typically exhibits 75% *head-to-tail* (*h–t*) configuration†. Poly(3,3′-dioctyl-2,2′-bithiophene) (PDOT$_2$)‡ is a regioregular (polymorphic) counterpart of POT. It consists of chains with a fully alternating . . . , *h–h*, *t–t*, *h–h*, . . . configuration as shown in figure 2. The crystalline structures of these two polymers are rather different. Whereas for both materials the structure can be described by a pseudo-orthorhombic unit cell, the lengths of the crystallographic axes differ: *a* axes: 20.3 ± 0.1 Å

† The sequence of connection points of the alkyl side chains to the thiophene backbone is described by the terms *head to tail* (*h–t*) and *head to head, tail to tail*, (. . . , *h–h*, *t–t*, *h–h*, . . .). Using the nomenclature introduced by Samuelsen and Mårdalen [11] where OT and TO mean octyl group connected to the left and right side of the thiophene ring respectively, a perfectly h–t coupled POT can be written [TO]$_n$ (figure 1) and the . . . , h–h, t–t, h–h, . . . coupled PDOT$_2$ can be written [(OT)$_1$(TO)$_1$]$_n$ (figure 2).
‡ PDOT$_2$ means two (D) octyl-thiophene (O) in a chain of two (2) thiophene (T) units. We find this abbreviation more descriptive than the correct IUPAC name.
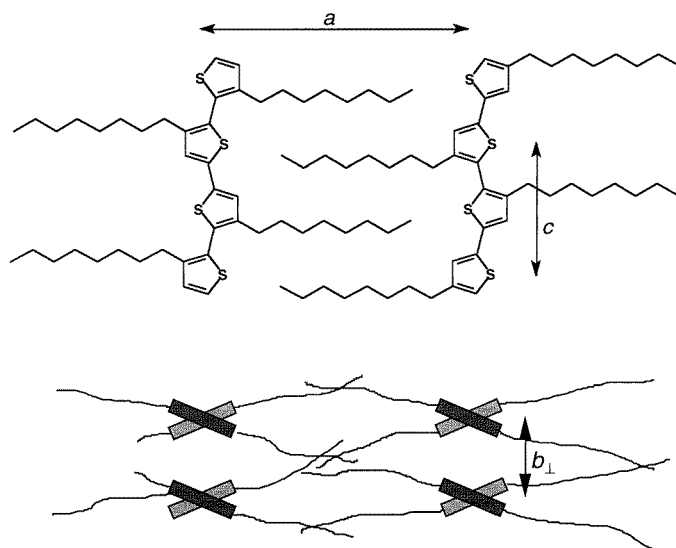
Figure 2. Simplified model for the PDOT$_2$ crystalline structure projected along the $b_\perp$ (upper) and c (lower) directions. The twist angle between adjacent thiophene rings shown in the lower figure should, according to calculations based on UV–vis spectroscopical studies, be about 40°.

and 14.6 ± 0.1 Å; and $b_\perp$ axes: 3.81 ± 0.05 Å and 4.42 ± 0.05 Å for POT and PDOT$_2$ respectively.

It is noteworthy that a second modification of the crystalline POT structure (type II) has been reported [13]. This structure is obtained from solutions after slow evaporation at high temperature (50 °C), and has lattice parameters very similar to those reported for PDOT$_2$. The closeness of the lattice parameters invites us to believe that the structure of PDOT$_2$ and POT type II could be similar.

The crystalline structure of PDOT$_2$ is not fully established, but a model has been advanced that involves an interchain twisting of the C–C bond connecting neighbouring thiophene rings in the h–h configuration [3, 14, 15]. The twisting is believed to be caused by a collective effect of the two side chains, and a twist angle of $\pm 40°$ has been deduced from spectroscopic measurements. This model corroborates well with the fact that PDOT$_2$ stays yellow at all temperatures, and, in contrast to POT, does not show any thermochromic effect.

3. Experiment

The POT used was provided by NESTE OY. It is in the form of a dark powder, polymerized with FeCl$_3$ as the coupling agent [16, 17]. The molecular weight M_w is about 34 500, corresponding to an average of about 200 monomer units per polymer chain, with a polydispersivity parameter $D = 3.1$.

The PDOT$_2$ was made at NTNU Chemistry Department in Trondheim, as previously reported [3, 14]. The material is in the form of a yellow powder, with molecular weight $M_w = 21\,600$ and $D = 4.3$.

The diffraction experiments were carried out at the ID9 beamline of the European Synchrotron Radiation Facility (ESRF), using a high pressure diamond anvil cell and a monochromatic x-ray beam of wavelength $\lambda = 0.6812$ Å.

Small amounts of polymer powder were loaded into the cell with silicon oil as the hydrostatic pressure medium. The pressure was monitored by the ruby luminescence method [18]. Studies were performed at room temperature only. Pressures up to more than 10 GPa were used. However, in subsequent high pressure studies by Lorenzen [19] at ESRF of other polymeric materials using silicon oil as pressure medium it was revealed that at pressures above 6 GPa non-hydrostatic processes set in. Therefore, mainly data for pressures below that value have been considered. Application of higher pressures also revealed a considerable hysteresis of the lattice parameters under decreasing pressures, or, in the case of PDOT$_2$, to complete irreversibility.

The diffracted x-rays were detected by a CCD camera coupled to an x-ray intensifier [20]. One-dimensional diffraction patterns were obtained by azimuthal integration of the two-dimensional images using the program *fit2d* [21]. This procedure was crucial for achieving diffraction patterns with a reasonable signal-to-noise ratio from these poorly scattering samples.

4. Results

4.1. POT

In figure 3 we show a set of diffraction patterns of POT at various applied pressures, as they appear after the azimuthal integration of the CCD-camera output. The scattering angle (2θ) is represented by the modulus of the scattering vector; $Q = 4\pi \sin\theta/\lambda$, where λ is the wavelength. It is noticed that the diffraction peaks reside on top of considerable background scattering mainly caused by the diamond windows of the high pressure cell.
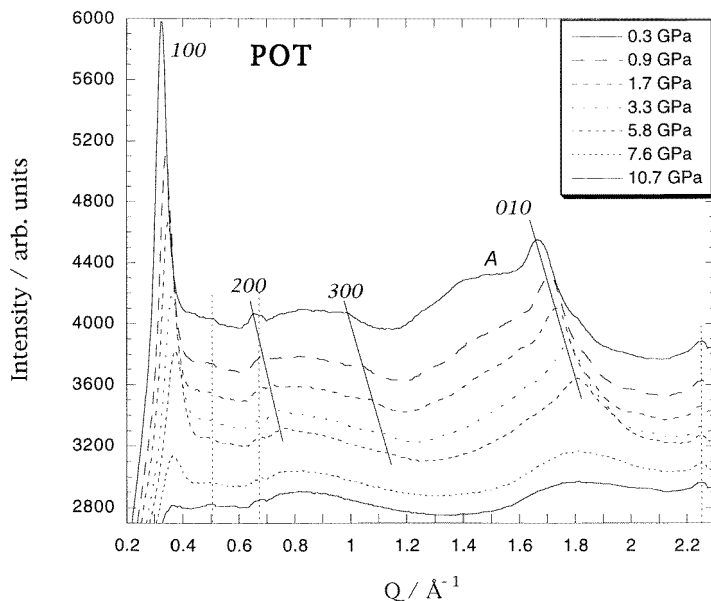

Figure 3. Diffraction pattern of POT under pressures from 0.3 to 10.7 GPa as a function of the scattering vector. Guidelines for the eye are drawn at the diffraction peaks 200, 300 and 010. The amorphous maximum is marked A and vertical dashed lines indicate scattering features not generated by the sample.

The well known diffraction pattern of POT [11] can be recognized, as shown by the indexing: a strong 100-reflection at low Q, followed by weak signatures of the 200 and 300; then an amorphous feature (at $Q = 1.4$ Å^{-1}) and an intermediate strength 010-peak at 1.65 Å^{-1}. These peaks are seen to be considerably influenced by the pressure, whereas two or three pressure-independent, spurious features are also seen. These are not known from previous measurements of POT, and are probably caused by the pressure cell or by something else in the experimental set-up and are not considered in the following.

The general behaviour under pressure is that the peaks move to higher angles, implying decrease of the lattice parameters. Also peak broadening and intensity decrease are observed. The actual peak positions were deduced from a curve fitting program (using the program package *ORIGIN*), and the associated lattice parameters are plotted in figure 5. As is seen the compression of the material comes to a saturation at increasing pressures. An exponential formula (see below) may describe the pressure dependence.

4.2. PDOT$_2$

Figure 4 shows the corresponding diffraction diagrams for PDOT$_2$. The first three peaks (at low pressures) are indexed 100, 200 and 300, whereas the peak at $Q = 1.45$ Å^{-1} is indexed 010. Diffuse, amorphous scattering occurs around 1.5 Å^{-1}, about the same position as for POT. All peaks move and broaden as the pressure is increased. The extracted lattice parameter behaviour is shown in figure 5. Also for PDOT$_2$ increased pressure leads to compression which tends to saturate.
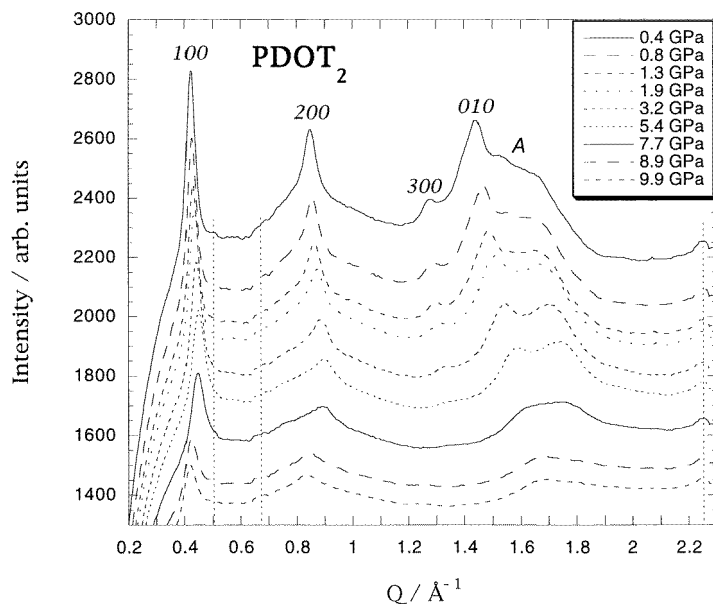

Figure 4. Diffraction pattern of PDOT$_2$ under pressures from 0.4 to 9.9 GPa. The diffraction peaks 200, 300 and 010 are indicated. The amorphous maximum is marked A and vertical dashed lines indicate scattering features not generated by the sample.
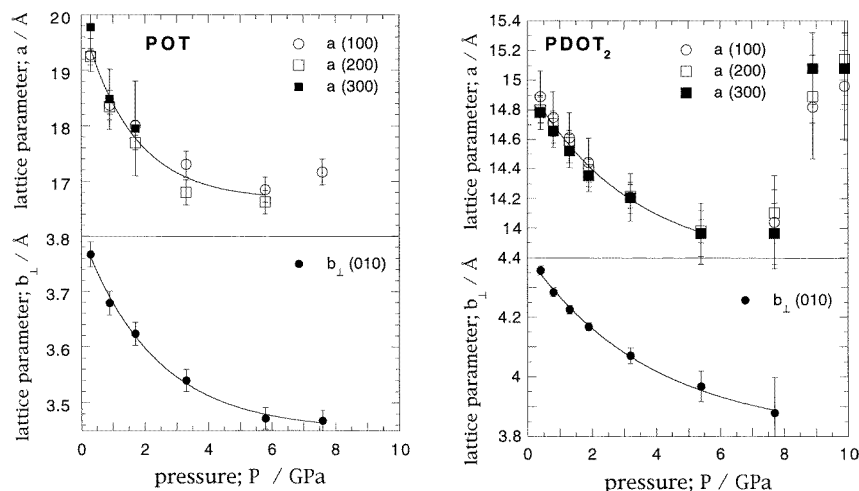
Figure 5. Unit cell parameters extracted from the diffraction patterns in figures 3 and 4 for POT and PDOT$_2$ respectively. The lattice parameters a shown in the upper curves are calculated from 100, 200 and 300 reflections with a reasonably good internal agreement. The exponential fits to the data are shown. For both the polymers the lattice parameters a show an unexpected increase for the highest pressures (see section 3).

4.3. Pressure dependence of unit cell parameters

For all the extracted lattice parameters (d) an exponential behaviour with pressure (P) is found, expressed as:

$$d = (d_0 - d_1)\,\mathrm{e}^{-cP} + d_1 \tag{1}$$

where d_0 is the lattice parameter at ambient pressure, d_1 the one at saturation and c is a parameter proportional to the compressibility. Given the exponential behaviour of d, the initial compressibility κ (for $P \to 0$) is:

$$\kappa = \lim_{P \to 0} \frac{\partial \ln d}{\partial P} = c\left(1 - \frac{d_1}{d_0}\right). \tag{2}$$

The numerical values obtained by fitting equation (1) to the a- and $b_\perp$-axis parameters of the two materials are shown in table 1. One will notice considerable anisotropy of the compressibilities as calculated from (2). Notice also the agreement between the fitted values for the lattice parameters at ambient pressure (d_0) and the corresponding values listed earlier in this paper.

5. Discussion

5.1. Compressibility and structure

The molecular structure of POT and PDOT$_2$ are not terribly different from each other (only the points of attachment of every second side chain along the polymer backbone), yet their crystalline structures differ a lot. The main difference is the topography of the main chains, being planar for POT and alternating twisted for PDOT$_2$. The twist is believed to be associated with a doubled C–S repulsion present in PDOT$_2$. Is it possible by application of hydrostatic pressure to force PDOT$_2$ into a more POT-like structure? Apparently not; at

Table 1. The calculated compressibility (κ) and the lattice parameters at ambient pressure (d_0) and at saturation (d_1) from fitting equation (1) to the extracted lattice parameters in figure 5 for POT and PDOT$_2$.

	Compressibility κ [GPa^{-1}]	d_0 (ambient P) [Å]	d_1 (saturation) [Å]
a (POT)	0.105	20.0	16.7
$b_\perp$ (POT)	0.039	3.80	3.44
a (PDOT$_2$)	0.022	14.94	13.62
$b_\perp$ (PDOT$_2$)	0.035	4.40	3.81

least for pressures below 8 GPa the two structures retain their own characteristics. But a certain approach between the length of the unit cell parameters of the two structures takes place.

The great difference between the compressibilities of the two polymers along the a-axes is noteworthy, implying that the side chains of POT are more deformable than those of PDOT$_2$ (making an angle to the a-axis). The large compressibility of a for POT corresponds to the observation of the same direction as the one with the largest thermal expansion [22]. The compressibilities along the b-axis, on the other hand, are about equal for the two compounds. For PDOT$_2$ the b-axis compressibility is roughly 50% higher than that of the a-axis, which indicates that the twist angle in fact does decrease as the pressure is increased. The compressibility in the c-direction could not be determined since no $l \neq 0$ reflection was measured.

The observed compressibilities along a and $b_\perp$ are of the same order of magnitude as observed for polyethylene (PE) where the directions perpendicular to the polymer chain direction have the compressibilities 0.117 and 0.075 GPa^{-1} [23]. PE is more compressible normal to the chain than along it (compressibility 0.003 GPa^{-1} along the chain). From their interchain geometry one expects the poly(thiophene)s also to be considerably less compressible along the chain direction than normal to it. As stated by Ito [23] this is a general rule for most polymers and means that bulk compressibility to a reasonable accuracy can be calculated as the sum of the compressibilities of the two directions normal to the polymer chain axis.

At saturation pressures the densities of the two compounds approach each other to some extent ($\rho_0 = 1.05$ g cm^{-3} (measured and calculated) and $\rho_1 = 1.40$ g cm^{-3} for POT, and $\rho_0 = 1.28$ g cm^{-3} (calculated) and $\rho_1 = 1.62$ g cm^{-3} for PDOT$_2$). Negligible compressibility in the c-direction is assumed for the calculation of the saturation density based on the same arguments as above.

For both materials the crystalline peaks broaden as the pressure increases. This is a feature observed in many polymers [19]. It can be related to the inherent inhomogeneity of the density of partially crystalline polymers. The denser crystallites will tend to slide into the less dense amorphous regions at high pressures, reducing their order during the motion and equalizing the density.

The behaviour of the amorphous part of the materials can be followed from the diffuse scattering maxima. For POT this maximum changes its Q-position more than the 010 diffraction peak. For PDOT$_2$ on the other hand, the 010 peak and the amorphous part seem to have about the same change in Q-position and thus about the same compressibility. It is not possible to give definite numbers because of the diffuseness, and because of the broadening of the peaks.

There exists good evidence that conjugated organic materials may undergo reactions like crosslinking under high pressure conditions [24]. Crosslinking might be one possible reason for the anomal increase of *a* both for POT and PDOT$_2$ at pressures around 8 GPa. Another possible reason is that the oil enters the polymer structure in an anisotropic fashion.

5.2. Relation to conductivity

There are many reports on electric conductivity studies under pressure of undoped and doped conjugated polymers. For undoped and lightly doped poly(alkyl-thiophene)s Isotalo *et al* [9] find that the conductivity increases with increasing pressures (up to 0.6 GPa). Iwasaki *et al* [7] find that the conductivity of poly(hexyl-thiophene) increases eightfold from ambient pressure to 2 GPa, where they see a maximum. Further increase to 5 GPa reduces the conductivity again by a factor of three.

The analysis given by Isotalo *et al* is of some interest here because the authors estimate the bulk compressibility for POT from their data. Using the Kivelson intersoliton hopping model they arrive at values in the range of 0.22–0.40 GPa^{-1}, based upon assumed values for the ratio of the 'distance between hopping centres' and the 'effective localization range'. Our data indicate that their estimate is off by only a factor of 1.5–3 if bulk data (sum of *a*- and *b*-axis data) are used. However, our data do not lend more support to this particular model over other models of the pressure dependence of the conductivity.

5.3. Spectral shifts

An interesting aspect of conjugated polymers is that their band structure is strongly dependent upon external conditions like temperature (thermochromic effect) and pressure. Since both temperature and pressure variations imply volume changes, it is of considerable interest to compare the two effects. Several studies have documented that the electronic properties of poly(alkyl-thiophene)s [6, 7] and other conjugated polymers [4, 5] are strongly influenced by external pressure. By absorption spectroscopy on poly(hexyl-thiophene) Iwasaki *et al* [7] observed an initial relative band gap decrease (from 1.97 eV at ambient pressure), followed by a minimum at 3 GPa, and an increase for higher pressures. Hess *et al* [6] observed that the thermochromic effect is suppressed at pressures above 1.4 GPa. They observed a steadily decreasing gap with increasing pressures up to 8 GPa, both with optical absorption and with photoluminescence. The initial slope obtained is 50% steeper than that of Iwasaki *et al*. Pressure studies of the absorption spectra of POT were recently published [25].

With our compressibility data we should now be in the position to check whether the thermochromic shift to higher gap energies and the pressure suppression of the gap energies are related phenomena, both linked to variation of the polymer geometry (i.e. expansion for the former case, compression for the latter). Since

$$\frac{\partial \ln W}{\partial \ln V} = \frac{\partial \ln W}{\partial P} \frac{\partial P}{\partial \ln V} = \frac{\partial \ln W}{\partial T} \frac{\partial T}{\partial \ln V} \tag{3}$$

one should compare

$$\frac{\kappa_{WP}}{\kappa_{VP}} \quad \text{with} \quad \frac{\kappa_{WT}}{\kappa_{VT}} \tag{4}$$

where $\kappa_{WP} = \partial \ln W / \partial P$ (relative shift of absorption peak maximum with pressure), $\kappa_{VP} = \partial \ln W / \partial T$ (volume compressibilities), $\kappa_{WT} = \partial \ln W / \partial T$ (relative thermochromic shift) and $\kappa_{VT} = \partial \ln V / \partial T$ (thermal volume expansion). The following data are available for non-stereoregular POT: $\kappa_{WP} = 0.05$ GPa^{-1} (for edge and peak) [25]; $\kappa_{VP} = 0.144$ GPa^{-1}

(summed values for the two directions) (this work); $\kappa_{WT} = 1.3 \times 10^{-4}$ K^{-1} (edge) [26, 27] and $\kappa_{WT} = 3.0 \times 10^{-4}$ K^{-1} (peak) [26, 27] and $\kappa_{VT} = 9.8 \times 10^{-4}$ K^{-1} [22]. From these data we obtain $\kappa_{WP}/\kappa_{VP} = 0.35$ and $\kappa_{WT}/\kappa_{VT} = 0.13$ (edge) and $\kappa_{WT}/\kappa_{VT} = 0.31$ (peak). One will notice the factor of 2.7 of disagreement for the edge shift data, which strongly indicates that the prime driving force for the spectral shifts is not the same under pressure and under temperature variations. This conclusion can also be inferred from the behaviour of the spectral peak *shapes*: whereas under pressure the absorption spectrum shifts practically unaltered as an entity, the thermochromic shift is predominantly of the peak maximum, which shifts about 2.7 times faster than the edge. In fact the *isobestic* behaviour of the thermochromic effect indicates that it can be interpreted as a composite of two spectra, 0.5 eV apart, consisting of one part belonging to *restricted* (ordered) regions, and another part belonging to *unrestricted* (disordered or 'melted') regions [27]. As the temperature increases the peak shift simply occurs because the fraction of disordered regions increases. The mechanism for the shift by pressure would be different. Both Iwasaki *et al* [7] and Hess *et al* [6] take the view that it is connected to an increase of *conjugation length* because pressure will suppress sidechain fluctuations. We would like to point out that an alternative model is one where the reduced interchain distances under pressure increases the wave function overlaps between chains, thus opening up the available space (in three dimensions) for the charge carriers. That would also explain qualitatively the initial increase of the electric conductivity under pressure. The suppression of the thermochromic transition for $P > 1.4$ GPa could then be due to higher compressibility for the disordered than for the ordered fraction, in qualitative agreement with our observations. Therefore, the density and the absorption spectrum of the disordered fraction would come close to that of the ordered fraction at higher pressure.

6. Conclusions

The linear compressibilities for the two forms of poly(octyl-thiophene) are of the same order of magnitude as for many other polymers. The compression approaches saturation at high pressures. The amorphous part of POT is qualitatively more compressible than the crystalline part. The linear compressibility of normal POT, which is known to have planar chains, is strongly anisotropic, being 2.5 times higher for the direction along the side chains (a-direction) than perpendicular to it ($b_\perp$-direction). Compressibility for the main chain direction (c-direction) could not be observed.

PDOT$_2$, which is believed to have non-planar main chains, with alternating twist along the chain, is less compressible and less anisotropic than POT. The difference between the two materials is related to the collective stiffness of the side chain systems.

The observed compressibility of POT is at some variance to values previously estimated from pressure studies of electric conductivity.

A comparison was made between the reported absorption spectral shifts due to applied pressure on the one hand and due to temperature variations on the other hand. It is concluded that the two types of shift cannot both be related only to the associated changes of the lattice geometry, but are due to different mechanisms. Whereas the thermochromic effect of POT is describable by a model of two phases whose relative weight varies with temperature, the shift due to pressure is related to an increased interchain wave function overlap, which qualitatively also can account for observed pressure effects on the electric conductivity. High pressure suppression of the thermochromic effect can be understood within this picture as being due to higher compressibility for the amorphous part.

Acknowledgment

References

[1] Inganäs O, Salaneck W R, Österholm J-E and Laakso 1988 *Synth. Met.* **22** 395
[2] Inganäs O 1997 *Handbook of Organic Conductive Molecules and Polymers* vol 3, ed H S Nalwa (New York: Wiley) p 785
[3] Fell H J, Samuelsen E J, Mårdalen J, Bakken E and Carlsen P H J 1995 *Synth. Met.* **69** 301
[4] Brillante A, Hanfland M, Syassen K and Hocker J 1986 *Physica* B **139/140** 533
[5] Hanfland M, Brilliante A, Syassen K, Stamm M and Fink J 1989 *J. Chem. Phys.* **90** 1930
[6] Hess B C, Kanner G S and Vardeny Z 1993 *Phys. Rev.* B **47** 1407
[7] Iwasaki K, Fujimoto H and Matsuzaki S 1994 *Synth. Met.* **63** 101
[8] Yoshino K, Nakao K, Onoda M and Sugimoto R 1989 *J. Phys.: Condens. Matter* **1** 1009
[9] Isotalo H, Ahlskog M and Stubb H 1992 *Synth. Met.* **48** 313
[10] Mårdalen J, Cerenius Y and Häggkvist P 1995 *J. Phys.: Condens. Matter* **7** 3501
[11] Samuelsen E J and Mårdalen J 1997 *Handbook of Organic Conductive Molecules and Polymers* vol 3, ed H S Nalwa (New York: Wiley) p 87
[12] Mårdalen J, Samuelsen E J, Gautun O R and Carlsen P H 1992 *Synth. Met.* **48** 363
[13] Prosa T J, Winokur M J and McCullogh R D 1996 *Macromolecules* **29** 3654
[14] Mårdalen J, Fell H J, Samuelsen E J, Bakken E, Carlsen P H J and Andersson M 1995 *Macromol. Chem. Phys.* **196** 553
[15] Luzny W, Rokita P, Zareba R and Kulszewicz-Bajer I 1995 *Synth. Met.* **75** 49
[16] Tamao K, Kodama S, Nakajima I, Kumada M, Minato A and Suzuki K 1982 *Tetrahedron* **38** 3347
[17] Österholm J-E, Laakso J, Nyholm P, Isotalo H, Stubb H, Inganäs O and Salaneck W R 1989 *Synth. Met.* **28** C435
[18] Piermarini G J, Bloch S, Barnett J P and Forman R A 1975 *J. Appl. Phys.* **46** 2774
[19] Lorenzen M in preparation
[20] Moy J P 1994 *Nucl. Instrum. Methods* A **348** 641
[21] Hammersley A P, Svensson S O, Hanfland M, Fitch A N and Hausermann D 1996 *High Pressure Res.* **14** 235
[22] Seeberg T 1997 *Diploma Thesis* The Norwegian University of Science and Technology (NTNU)
[23] Ito T 1979 *High-Pressure Science and Technology* vol 1, ed K D Timmerhaus and M S Barber (New York: Plenum) p 482
[24] Nicol M and Yin G Z 1984 *J. Physique Coll.* **45** C8 164
[25] Kaniowski T, Niziol S, Sanetra J, Trznadel M and Pron A 1998 *Synth. Met.* **94** 111
[26] Fell H-J, Samuelsen E J, Mårdalen J and Carlsen P H 1994 *Synth. Met.* **63** 167
[27] Konestabo O R, Samuelsen E J and Fell H J to be published
See also [2]